Direct Spectroscopic Observation of Elementary Excitations in Superfluid He Droplets

M. Hartmann, F. Mielke, J. P. Toennies, and A. F. Vilesov
Max-Planck-Institut für Strömungsforschung, Bunsenstrasse 10, D-37073 Göttingen, Germany

G. Benedek
Istituto Nazionale di Fisica della Materia, Dipartimento di Fisica dell'Università, via Celoria, I-20133 Milano, Italy

(Received 9 February 1996)

The absorption spectra of the electronic $S_1 \leftarrow S_0$ transition of glyoxal molecules ($C_2H_2O_2$) embedded in He droplets ($\approx$5500 atoms) show well-resolved vibronic bands with a width < 0.5 cm^{-1}. The phonon wings at higher frequencies have distinct gaps amounting to $\Delta E = 8.1$ K followed by a small maximum at 14.8 K. The phonon wing shape agrees with a theoretical simulation based on the dispersion curve of elementary excitations in bulk He II, providing the first evidence for superfluidity in the finite-sized He droplets. [S0031-9007(96)00383-3]

PACS numbers: 67.40.Yv, 33.20.Kf, 67.40.Db

A number of recent theoretical studies predict that ^{4}He clusters with more than about 64 atoms are superfluid with a transition temperature which is somewhat lower than the bulk λ-point temperature $T_\lambda = 2.2$ K [1–3]. So far, however, there is no direct experimental evidence for superfluidity in these nanosize liquid particles. Recently it has been possible to observe a very sharp rovibrational spectrum of single SF_6 molecules located in the interior of He droplets ($N > 1000$ atoms) which were produced in free jet expansions [4,5]. From this the rotational temperature was found to be $T = 0.37 \pm 0.05$ K [5] in good agreement with theoretical predictions [6]. In addition, infrared spectra of SF_6 dimers indicate that these larger entities can also rotate freely in the He droplets [7].

In the bulk the most direct evidence for superfluidity comes from neutron diffraction experiments which indicate sharp elementary excitations with a dispersion characterized by a maximum at $E_{\max} = 13.7$ K ($Q_{\max} = 1.10$ Å^{-1}) called a maxon and the well known roton minimum at $E_{\mathrm{rot}} = 8.65$ K ($Q_{\mathrm{rot}} = 1.91$ Å^{-1}) [8]. As first pointed out by Landau the sharp excitations at the roton minimum enable the fluid to flow unhindered at velocities below about 58 m/s which is the most prominent manifestation of superfluidity. This critical velocity could so far only be observed for negative ions which were found to move without friction in liquid helium at $P = 25$ atm and $T = 0.4$ K [9]. Two-phonon Raman spectroscopy in bulk helium also has been shown to provide information on the elementary excitations [10]. In the quest for more direct spectroscopic probes of superfluidity several groups have developed sophisticated techniques to levitate atoms in liquid helium [11–14]. Up to now only broad lines of several cm^{-1} width could be observed. A recent study of the electronic spectra of Na_2 attached to the surface of He droplets reveals vibronic bands consisting of a sharp zero phonon line (ZPL) and an intense broad phonon wing (PW) [15]. In this system multiphonon processes appear to dominate the spectra and conceal the elementary excitations of the droplet.

To circumvent these difficulties we have undertaken the first spectroscopic experiments with a simple organic molecule. Glyoxal ($C_2H_2O_2$) was chosen since its visible spectroscopy has been studied both as a free molecule and in cryomatrices [16,17]. Compared to the alkali metals glyoxal is readily solvated by helium. Moreover, the electronic ($S_1 \leftarrow S_0$) excitation has an intravalent $n\pi^*$ character so that the electron-phonon coupling to the surrounding medium is sufficiently weak to assure narrow lines, yet just strong enough to allow for phonon excitation.

The molecular beam laser apparatus is essentially similar to that used in the previous works [4,5]. The He droplet beam is formed by expanding He gas from a 5 μm thin walled orifice operated at a stagnation pressure of $P_0 = 20$ bar and a temperature of $T_0 = 14$ K. From the previous experiments it is known that these droplets have a mean size of 5500 atoms [18]. Glyoxal, which was prepared following standard procedures [16], was admitted at a pressure of approximately 10^{-5} mbar into a 2 cm long scattering cell located 30 cm from the source. Following pickup of a glyoxal molecule the doped droplets in the beam are detected on the mass of a COH^+ fragment ion by a quadrupole mass spectrometer with the electron impact ionizer located 142 cm from the source. The beam of a pulsed dye laser (repetition rate 57 Hz) is directed antiparallel to the droplet beam and interacts with the doped droplets over a distance of 112 cm as they pass from the cell to the ionizer. Photon absorption after a laser pulse leads to a transient decrease of the mass spectrometric signal (up to $\sim$30%) due to the evaporation of several hundred He atoms. Because of the long interaction distance and the low beam velocity of about 340 m/s the depletion signal lasts for approximately 3.5 ms after a laser pulse.

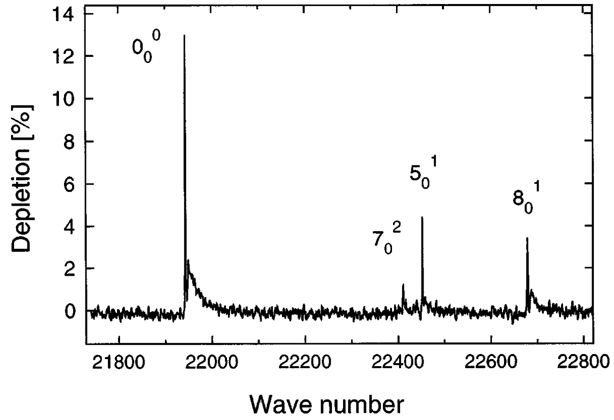

FIG. 1. Absorption spectrum of glyoxal embedded in He droplets, recorded at laser output energy of 1.1 mJ/phase. The assignment of the vibronic bands is indicated.

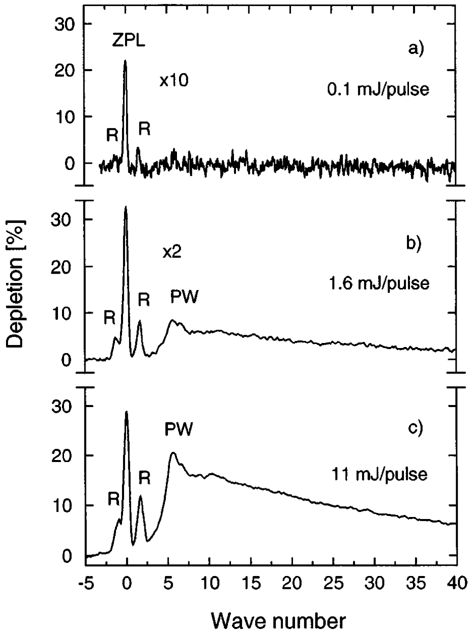

FIG. 2. Absorption spectra of glyoxal in the range of the 0_0^0 band, measured for different laser output energies: (a) $E = 0.1$ mJ/pulse, (b) $E = 1.6$ mJ/pulse, (c) $E = 11$ mJ/pulse. Zero energy corresponds to the maximum of the ZPL at 21 942.8 cm^{-1}. R denotes the rotational structure of the ZPL.

Figure 1 shows an overview absorption spectrum of glyoxal in a He droplet in the range of 21 730 to 22 820 cm^{-1}. The spectrum consists of four very sharp ZPL each having a weak broader feature on its blue side which is ascribed to a PW. The lines can be identified as vibronic transitions between the ground state S_0 and the first excited singlet state S_1 of glyoxal due to the close similarity of the observed spectrum and the corresponding free jet expansion LIF (laser-induced fluorescence) spectrum [16]. The position of the 0_0^0 band of glyoxal in a He droplet is found to be redshifted by 30.6 cm^{-1} relative to the corresponding band origin of the free molecule [16]. The vibrational frequencies of glyoxal (S_1) in He were found to be slightly larger than in the free molecule [16] by 4.6, 0.1, and 0.9 cm^{-1} for the ν_7 (torsion), ν_5 (CCO bend), and the ν_8 (CH wag) modes, respectively. Compared to our spectrum the absorption spectrum of glyoxal in a solid Ar matrix consists of much broader lines ($\Delta\nu \approx 200$ cm^{-1}) which conceal the ZPL components [17].

In Fig. 2 three spectra in the range of the 0_0^0 band are displayed for different laser ouput energies: (a) 0.1 mJ/pulse, (b) 1.6 mJ/pulse, and (c) 11 mJ/pulse. The intensity of the PW increases with increasing pulse energy, whereas the ZPL transition saturates. The ZPL fine structure is ascribed to the rotational structure of the transition and will be discussed elsewhere [19]. Additional measurements with an intracavity etalon reveal a linewidth of the ZPL of less than 0.1 cm^{-1}.

The PW reflects the excitation of phonons in the He droplets accompanying photon absorption by the glyoxal molecule. From Fig. 2(c) it is seen that the intensity of the PW is very small at $E < 4$ cm^{-1} (5.8 K), where E is measured with respect to the ZPL. The intensity then rises dramatically and reaches its maximum at $E = 5.6$ cm^{-1} (8.1 K). A second, less pronounced maximum can also be safely distinguished at $E = 10.3$ cm^{-1} (14.8 K). At still higher energies the intensity gradually decreases without any additional structure. The phonon wings of the other vibronic bands exhibit the same distinct gap between ZPL and PW and the maximum of the PW at $\approx$8.1 K. The gap has been found to be independent of the droplet size for $1000 < N < 15\,000$ atoms.

As far as we are aware a gap between a well separated ZPL and PW has not been observed previously in classical solutions or cryosolutions [20]. One reason is that at the relatively high temperatures ($T \geq 70$ K) usually needed to keep the matrix liquid the medium will have a high density of phonon states. These tend to reduce the excited state lifetime and smear out the PW line shape. Moreover, in classical liquids only the low Q region of the longitudinal branch is reasonably sharp [21] and a gap is not expected. In contrast, liquid He droplets at $T \approx 0.37$ K, expected to be superfluid, provide a coherent environment. As a result they resemble more a cold solid matrix without inhomogeneous broadening, rather than a classical liquid.

The spectral shape of the PW can be analyzed using the theory of impurity spectra in solid matrices [22]. According to this theoretical approach the absorption cross section vs transition frequency ω can be written as

$$\sigma(\omega) = \frac{4\pi^2\omega}{\hbar c}|M_{eg}|^2 G(\omega - \omega_{eg}), \qquad (1)$$

where M_{eg} is the matrix element of electronic excitation of a molecule. The subscripts e and g refer to the electronically excited and the ground state of the molecule, respectively. $G(\omega)$ is a normalized spectral shape function given by

$$\begin{aligned} G(\omega) &= \sum_{\{n_Q\}} \left[\int d\vec{r}\,\Psi^{(e)}_{\{n_Q\}}(\vec{r})\Psi_0^{(g)*}(\vec{r}) \right]^2 \\ &\quad \times \delta\left(\omega - \sum_Q n_Q \omega_Q\right) \\ &= e^{-S}\sum_n (S^n/n!)B_n(\omega)\,, \end{aligned} \tag{2}$$

where the cluster microscopic wave functions $\Psi_0^{(g)}$ and $\Psi^{(e)}_{\{n_Q\}}$ refer to the cluster ground state for the molecule in the ground state and to the cluster excited state (n_Q quanta in each normal mode of frequency ω_Q and wave number Q) for the molecule in the excited state, respectively. Integration is over the N position vectors $\vec{r} = \{\vec{r}_1, \vec{r}_2, \ldots, \vec{r}_N\}$ of the He atoms. The spectral function is expanded over the n-excitation components $B_n(\omega)$ (normalized to unity), where $B_0(\omega) = \delta(\omega)$ is the zero-excitation line and

$$B_n(\omega) = \int d\omega' B_{n-1}(\omega')B_1(\omega - \omega')\,. \tag{3}$$

The one-excitation spectrum $B_1(\omega)$ and the Huang-Rhys factor S can be calculated by assuming that the molecule is a sphere of radius R_0 located at the cluster center and that its excitation yields a sudden shift $R_0 \rightarrow R_0 + \Delta$ of its boundary with a volume increase of $\delta V = 4\pi R_0^2\Delta$. $\Psi_0(\vec{r})$ and $\Psi_{1Q}(\vec{r})$ (where the index $1Q$ refers to single excitation wave functions) are replaced with the respective Feynman macroscopic wave functions $\psi(R) = \rho^{1/2}(R)e^{i\phi}$ and $f_{1Q}(R)\psi(R)$. $\rho(R)$ is the cluster density, ϕ is a phase related to the velocity field by $\vec{v}(\hbar/m)\Delta\phi$, and $f_{1Q}(R)$ is the one-excitation wave function [2]. We obtain

$$B_1(\omega) = \frac{(\rho_0\delta V)^2}{4S}\sum_Q |f_{1Q}(R_0)|^2 e^{-Q^2/2\beta^2}\delta(\omega - \omega_Q)\,, \tag{4}$$

and S is given by the condition $\int B_1(\omega)\,d\omega = 1$. In Eq. (4) ρ_0 is the He density near the boundary so that the electron-excitation coupling strength $\rho_0\delta V$ represents the number of He atoms which are displaced at the molecule boundary during the electronic transition. $\Psi(R)$ is assumed to decay inside the molecule boundary like $\mathrm{erfc}[\beta(R - R_0)]$ in order to account for the softness of the molecule-He repulsive potential. Only s waves are considered since these are the only ones having an appreciable intensity near the molecule boundary, i.e., in the vicinity of the cluster center,

$$f_{1Q}(R) = A\,\frac{\sin QR}{R} + B\,\frac{\cos QR}{R}\,, \tag{5}$$

where A, B, and the set of allowed Q values are obtained from normality and the boundary conditions $f_{1Q}(R_c) = 0$ (R_c = cluster radius) and $f'_{1Q}(R_0) = 0$.

The spectral shape of a PW was simulated using Eq. (2). The calculations of Refs. [2,3] indicate that the elementary excitation dispersion curves of large He droplets are very similar to those in the bulk. Thus, $\omega(Q)$ was first taken from the dispersion curve for bulk He II [8] for $Q < 2.4$ Å^{-1}. For $Q > 2.4$ Å^{-1} $\omega(Q)$ was approximated by the parabolic dependence of a free particle. $\beta = 1.1$ Å^{-1} was obtained from a best fit to the experimental spectrum. This value agrees well with the thickness of the He boundary near impurities calculated in [23]. $f_{1Q}(R_0)$ is proportional to Q in the limit of $R_0 \ll R_c$ according to Eq. (5). From Eq. (2) it is seen that $e^{-S} = I_{\mathrm{ZPL}}/(I_{\mathrm{PW}} + I_{\mathrm{ZPL}})$, where I_{ZPL} and I_{PW} are the integrated intensities in the ZPL and PW, respectively. $e^{-S} \approx 0.2$ was estimated from the spectrum Fig. 2(a).

Figure 3(a) displays the simulated one-excitation spectrum $B_1(E)$ and the resulting multiphonon contribution up to $n = 5$ according to Eqs. (2)–(4). $B_1(E)$ shows two distinct maxima at $E_{\mathrm{rot}} = 8.7$ K and $E_{\max} = 13.7$ K which reflect the high density of excitation states in the vicinity of the dispersion curve extrema. Figure 3(b) shows the convolution of this spectrum with a Lorentzian line-shape function (FWHM 1.4 cm^{-1} = 2 K). The ap-

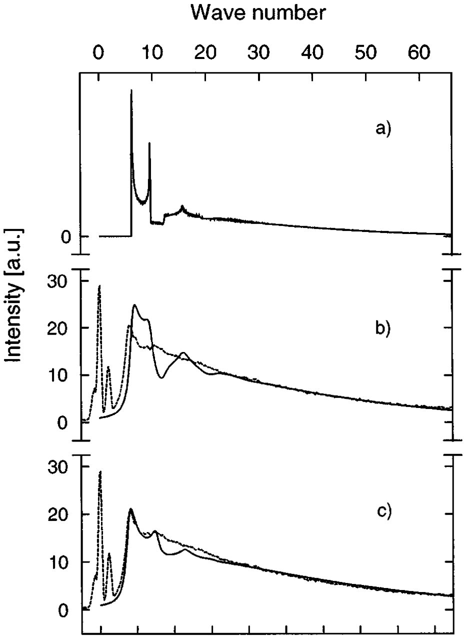

FIG. 3. (a) Calculation of the multiphonon spectrum from the dispersion curve for bulk He II according Eqs. (2)–(4); (b) comparison between the measured spectrum (dashed line) of the PW of glyoxal in He droplets and the simulation (a), convoluted with a Lorentzian (FWHM = 2 K); (c) same as (b) with a modified dispersion curve for the He droplets.

paratus linewidth is determined by the laser bandwidth of $\Delta\nu = 0.5$ cm^{-1}. We also expect an intrinsic broadening of the phonon spectrum at energies above $E = 7.2$ K due to the continuum of dissociating states. The convoluted spectrum compares satisfactorily with the experimental spectrum of the 0_0^0 band from Fig. 2(c). In particular, the sharp rise in intensity at $E \approx 6$ can be reproduced which shows that the intrinsic half width of the droplet excitations near the roton minimum is less than 2 K. The sharpness of the single excitation spectrum in the bulk is known to be characteristic for the superfluid state. The linewidth of the roton excitation in bulk liquid He above T_λ being 9 K [24] is considerably larger.

The convoluted spectrum also shows a maximum at $E = 9.5$ K near the observed maximum of the PW at $E = 8.1$ K. The upward shift with respect to E_{rot} is due to the convolution with the Lorentzian. The weak second maximum in the experimental spectrum at $E = 14.8$ K can hardly be interpreted as a two-roton process because this would imply a binding energy with respect to the two-roton energy of $E = 17.3$ K in the bulk of 2.5 K which is greater than the accepted value of 0.22 K [10]. More likely it can be assigned to the maxon. However, the observed roton and maxon energies in the cluster are somewhat below and above the respective bulk energies from neutron data. Recent quantum-chemical calculations [25] of the glyoxal-He potential predict a minimum of 41 cm^{-1} for a sandwich geometry and about 20 cm^{-1} for the two minima in the molecular plane. It is known that the molecule potential leads to an increase in the density of helium near the molecule [23], which is expected to soften the roton and stiffen the maxon as measured with increasing pressure in bulk liquid He where at $P = 20$ bar $E_{\mathrm{rot}} = 7.4$ K and $E_{\max} = 14.8$ K [26]. A slightly modified dispersion curve for the doped droplets with $E_{\mathrm{rot}} = 7.8$ K and $E_{\max} = 15.1$ K leads to a much better agreement between simulation and experiment as shown in Fig. 3(c).

The present study provides the first experimental evidence for superfluidity of He droplets. The observation of sharp ZPLs accompanied by rather weak PWs removed by a sharp gap in He droplets suggests, moreover, that these droplets can be used as an ultracold and homogeneous medium for electronic spectroscopy of large molecules. Work is presently underway to study spectra of more complex molecules in He droplets.

The authors are grateful to P. Hobza for calculating the glyoxal-He binding energies and to Ch. Parmenter and G. J. Kroes for information on the glyoxal-He potential. They thank T. Winkler for his help in glyoxal preparation. A. V. and M. H. thank the Deutsche Forchungsgemeinschaft for financial support.

[1] B. P. Sindzingre, M. L. Klein, and D. M. Ceperley, Phys. Rev. Lett. **63**, 1601 (1989).
[2] M. V. R. Krishna and K. B. Whaley, J. Chem. Phys. **93**, 746 (1990).
[3] S. A. Chin and E. Krotschek, Phys. Rev. B **45**, 852 (1992).
[4] R. Fröchtenicht, J. P. Toennies, and A. F. Vilesov, Chem. Phys. Lett. **229**, 1 (1994).
[5] M. Hartmann, R. E. Miller, J. P. Toennies, and A. F. Vilesov, Phys. Rev. Lett. **75**, 1566 (1995).
[6] D. M. Brink and S. Stringari, Z. Phys. D **15**, 257 (1990).
[7] M. Hartmann, R. E. Miller, J. P. Toennies, and A. F. Vilesov, Science (to be published).
[8] R. A. Cowley and A. D. B. Woods, Can. J. Phys. **49**, 177 (1971).
[9] D. R. Allum, P. V. E. McClintock, A. Phillips, and R. M. Bowley, Philos. Trans. R. Soc. London A **284**, 179 (1977).
[10] C. A. Murray, R. L. Woerner, and T. J. Greytak, J. Phys. C **8**, L90 (1975).
[11] R. E. Boltnev *et al.*, Chem. Phys. **189**, 367 (1994).
[12] Y. Takahashi, K. Sano, T. Kinoshita, and T. Yabuzaki, Phys. Rev. Lett. **71**, 1035 (1993).
[13] G. zu Putlitz and M. R. Beau, *Topics in Applied Physics* (Springer, Berlin, 1992); Vol. 70.
[14] J. H. M. Beijersbergen, Q. Hui, and M. Takami, Phys. Lett. A **181**, 393 (1993).
[15] F. Stienkemeier, J. Higgins, W. E. Ernst, and G. Scoles, Phys. Rev. Lett. **74**, 3592 (1995); Z. Phys. B **98**, 413 (1995); J. Chem. Phys. **102**, 615 (1995).
[16] E. P. Peyroula and R. Jost, J. Mol. Spectrosc. **121**, 117 (1987).
[17] L. J. IJzendoorn *et al.*, J. Chem. Phys. **85**, 1812 (1986).
[18] M. Lewerenz, B. Schilling, and J. P. Toennies, Chem. Phys. Lett. **206**, 381 (1993).
[19] M. Hartmann, F. Mielke, J. P. Toennies, and A. F. Vilesov (to be published).
[20] *Molecular Cryospectroscopy*, edited by R. J. H. Clark and R. E. Hester, Advances in Spectroscopy Vol. 23 (Wiley & Sons, Singapore, 1995).
[21] A. A. van Well and L. A. de Graaf, Phys. Rev. A **32**, 2396 (1985).
[22] M. H. L. Pryce, in *Phonons in Perfect Lattices and in Lattice with Point Imperfections* (Oliver & Boyd, Edinburgh and London, 1966), p. 403.
[23] F. Dalfovo, Z. Phys. D **29**, 61 (1994).
[24] W. G. Stirling and H. R. Glyde, Phys. Rev. B **41**, 4424 (1990).
[25] P. Hobza (private communication).
[26] E. F. Talbot, H. R. Glyde, W. G. Stirling, and E. C. Svensson, Phys. Rev. B **38**, 11 229 (1988).